SLAC-PUB-2009
September 1977
(T/E)

LARGE TRANSVERSE MOMENTUM PHENOMENA*

Stanley J. Brodsky
Stanford Linear Accelerator Center
Stanford University, Stanford, California 94305

I. Introduction

Since a finite fraction of the momentum of hadrons is carried by elementary quark fields, one expects that hard collisions involving these constituents can produce particles at very large transverse momentum. In fact, the phenomenological features which have emerged from the recent Fermilab and ISR experiments—particularly the jet structure and power-law scaling behavior of the inclusive cross sections—appear to be consistent with the properties expected from underlying elementary two-body scattering subprocesses. It is particularly significant that the quantum numbers of the leading particles are strongly correlated with the quantum numbers of the incident hadrons (e.g., the decreasing K^-/K^+ and $\bar{p}/p$ ratios at large $x_T = 2p_T/\sqrt{s}$ in pp collisions) indicating that the valence quarks themselves are transferred to large p_T. The crucial question is how they get there!

The most obvious candidate for the hard scattering process is quark-quark scattering, as first discussed by Berman, Bjorken, and Kogut.[1] It is clear that this mechanism must contribute to the large p_T cross section at some level—if not by a basic hadronic force, then by electromagnetic or weak interactions. Still, it is difficult to reconcile an elementary quark-quark scattering mechanism with present ISR and FNAL data (involving transverse momentum below ~8 GeV) for the following reasons:

(1) The results of the new British-French-Scandinavian[2] ISR experiment for pp → charged hadrons at $\theta_{c.m.} = 90^\circ$ (see Fig. 1) show that K^-

*Work supported by the Energy Research and Development Administration.

(Invited talk presented at the VIII International Symposium on Multiparticle Dynamics, Kaysersberg, France, June 12-17, 1977.)

and $\bar{p}$ beyond p_T = 3 GeV are preferentially balanced by positive particles on the away side, whereas within errors there is no charge correlation for K^+, $\pi^\pm$ or p triggers. Such charge correlations between the trigger and away side are not expected in valence quark-quark (or gluon) scattering models.[3] The BFS data also show that the momentum accompanying the trigger particle on the same side does not increase perceptably with the K^- trigger momentum (see Fig. 2), again contrary to what one expects from the scattering and fragmentation of valence quarks.

(2) The scaling behavior of the 90° inclusive cross sections, $d\sigma/d^3p/E \cong p_T^{-8} f(x_T)$ for meson production, and $\cong p_T^{-12} f(x_T)$ for proton production over a wide kinematical range,[4] implies strong, nonperturbative scale breaking corrections to the expected $\alpha_s^2(p_T^2) p_T^{-4} f(x_T)$ form.[5] In the Field and Feynman[6] model, the quark-quark cross section is fit to the form $d\sigma/dt = C/st^3$ (or C/su^3) in order to fit the

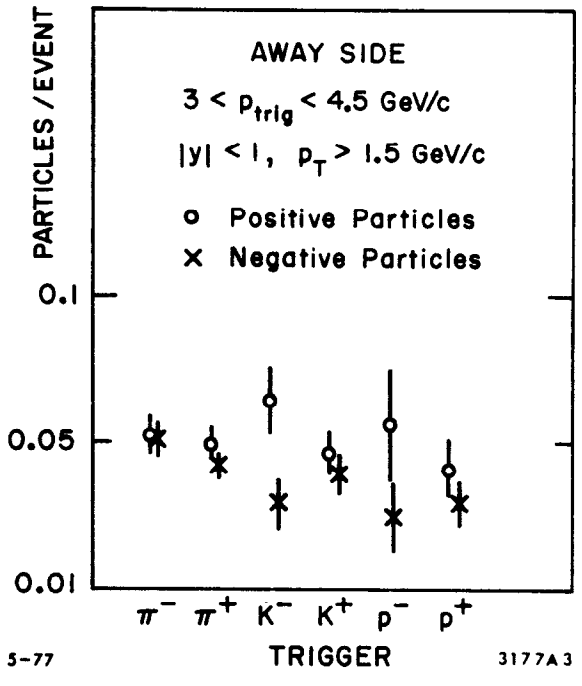

Fig. 1. Number of fast positive and negative particles on the side away from a 90° trigger for various trigger types. From Ref. 2.

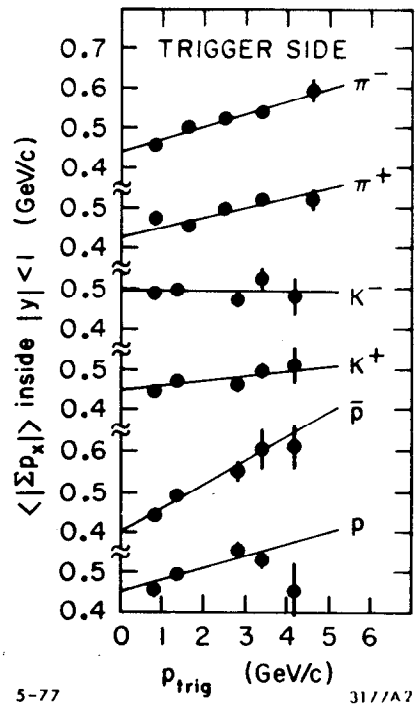

Fig. 2. The total momentum of particles along the 90° trigger particle for various charged particles. From Ref. 2.

scaling behavior and angular dependence of meson production data; an additional mechanism is then required for baryon production. Further, the normalization of the cross section requires C to be huge (2.3 b GeV$^6 = 5800$ GeV^4) due to quark fragmentation, and the angular form is indicative of fermion ($J = 1/2$) rather than boson exchange.

(3) Quite careful calculations of the sum of the quark-quark scattering QCD terms using the nominal value of $\alpha_s \sim 0.2$ to 0.3 indicates that the QCD contribution lies an order of magnitude below the data for $p_T < 6$ GeV for single particle production in the ISR, FNAL energy range. Furthermore, using Eq. (3.4) and[7]

$$\frac{d\sigma}{dt}(q_a q_b \to q_a q_b) = \frac{4}{9}\frac{\pi\alpha_s^2}{s^2}\left[\frac{s^2+u^2}{t^2} + \delta_{ab}\left(\frac{s^2+t^2}{u^2} - \frac{2}{3}\frac{s^2}{ut}\right)\right] \tag{1.1}$$

for the (color-averaged) quark-quark cross section, one obtains ($\theta_{c.m.} = 90^o$, $x_T = p_T/p_T^{max}$)

$$\frac{d\sigma}{d^3p/E}(pp \to "q" X) \cong 3\,\alpha_s^2\frac{(1-x_T)^7}{p_T^4} \tag{1.2}$$

At $s = 400$ GeV, $p_T = 5$ GeV, with $\alpha_s = 0.3$, this gives a jet cross section[8] ~ 1.5 nb/GeV^2, small compared to the jet cross section ~ 15 to 20 nb/GeV^2 recently reported by the E260 Fermilab collaboration.[9]

(4) A most critical point is that the $qq \to qq$ model does not account for exclusive large p_T processes. The natural prediction is

$$\frac{d\sigma}{dt}(pp \to pp) \cong N_{coh}^2\,\frac{d\sigma}{dt}(qq \to qq)\,F_p^4(t) \tag{1.3}$$

where N_{coh} is the number of coherent terms. Using Eq. (1.1) and $N_{coh} = 9$, one predicts (in GeV units)[10]

$$\frac{d\sigma}{dt}(pp \to pp)\left|_{(\theta_{c.m.}=90^o)}\right. = \frac{9.4\times10^3}{s^{10}}\alpha_s^2 \tag{1.4}$$

This is consistent with the observed fixed angle scaling behavior $s^{-9.7\pm0.5} f(\theta_{c.m.})$, but the experimental cross section normalization fits

$$\frac{d\sigma}{dt}(pp \to pp)\Big|_{(\theta_{c.m.}=90^o)} = \frac{1.3\times10^9}{s^{10}} \tag{1.5}$$

requiring $\alpha_s = 370$. Similarly, the Field-Feynman form for $d\sigma/dt\,(qq \to qq)$ yields a cross section four orders of magnitude too small at $s = 20$ GeV^2, $\theta_{c.m.} = 90^o$. The $qq \to qq$ terms also yield the wrong angular distributions for pp scattering, predicting that the effective Regge trajectory $\alpha(t) \to 1$ at large $-t$ (for gluon exchange) or $\alpha(t) \to 1/2$ at large $-t$ (for the F-F model). The data indicates that $\alpha(t)$ falls to a negative value, below -1, at large spacelike t. Furthermore since gluons do not carry flavor, it is difficult to understand why charge exchange reactions at large t are comparable in size to elastic reactions.

In the Constituent Interchange Model (CIM), developed by Blankenbecler, Gunion, and myself,[12] the basic hard-scattering subprocesses are postulated to be quark-hadron interactions (e.g., $qM \to qM$, $qB \to qB$, and the reactions related by crossing, $q\bar{q} \to MM$, $q\bar{q} \to B\bar{B}$, etc.). Since the high p_T hadrons can be formed directly in these subprocesses, the CIM cross sections, unlike quark and gluon jet subprocesses, are not suppressed by trigger bias (an effect which typically reduces quark fragmentation cross sections by two orders of magnitude).

The calculations in the CIM assume that there is a finite coupling of the hadronic states to valence quark fields, $|M\rangle_V = |q\bar{q}\rangle$, $|B\rangle_V = |qqq\rangle$, and that the underlying quark-quark interaction kernels are asymptotically scale-free. Thus, modulo possible logarithmic corrections, the CIM is consistent with QCD. A simple calculation

for spin 1/2 quark-hadron scattering at large t and u gives (see Fig. 3a)

$$\frac{d\sigma}{dt}(u\pi^+ \to u\pi^+) = \pi\alpha_M^2 \frac{-1}{su^3} \tag{1.6a}$$

(corresponding to elementary spin 1/2 exchange at fixed u) and

$$\frac{d\sigma}{dt}(up \to up) \cong \pi\alpha_B^2 \frac{1}{s^2u^4} \tag{1.6b}$$

where $\alpha_M^2 = \frac{1}{3}\frac{g^2}{4\pi}$ is the effective meson-quark-antiquark vertex coupling constant (units of mass-squared), and g is proportional to the Bethe-Salpeter wave function $\psi(x=0)$ at the origin and the QCD $qq \to qq$ coupling constant. Equations (1.6) give cross sections for a quark of specific color. For simplicity, we will assume SU(3) symmetry. By crossing we also have

$$\frac{d\sigma}{dt}(u\bar{u} \to \pi^+\pi^-) = \frac{1}{2}\pi\alpha_M^2 \frac{-t}{s^2u^2}\ , \tag{1.7}$$

etc. The calculations in the CIM are consistent with the dimensional counting rules.[13] We emphasize that the quark-hadron scattering amplitudes contribute in any quark model since their normalization is already fixed from the hadronic Bethe-Salpeter wave functions, elastic form factors, momentum sum rules for structure functions, etc. In fact, as we shall review here, the CIM predictions are consistent with not only the scaling laws and angular dependence of the measured exclusive and inclusive large p_T cross sections, but also their normalization.[14] The strong charge correlations between the trigger and away side jet found by the BSF group are also natural in the CIM approach.

II. The Structure of the CIM—Exclusive Reactions[13,14]

Given the basic building block, Eq. (1.6), for quark-hadron scattering, it is easy to construct a theory of large p_T exclusive processes which should be valid whenever valence quark effects dominate. Figure 3 indicates how one can proceed from the standard quark parton model representations of the elastic electron scattering and

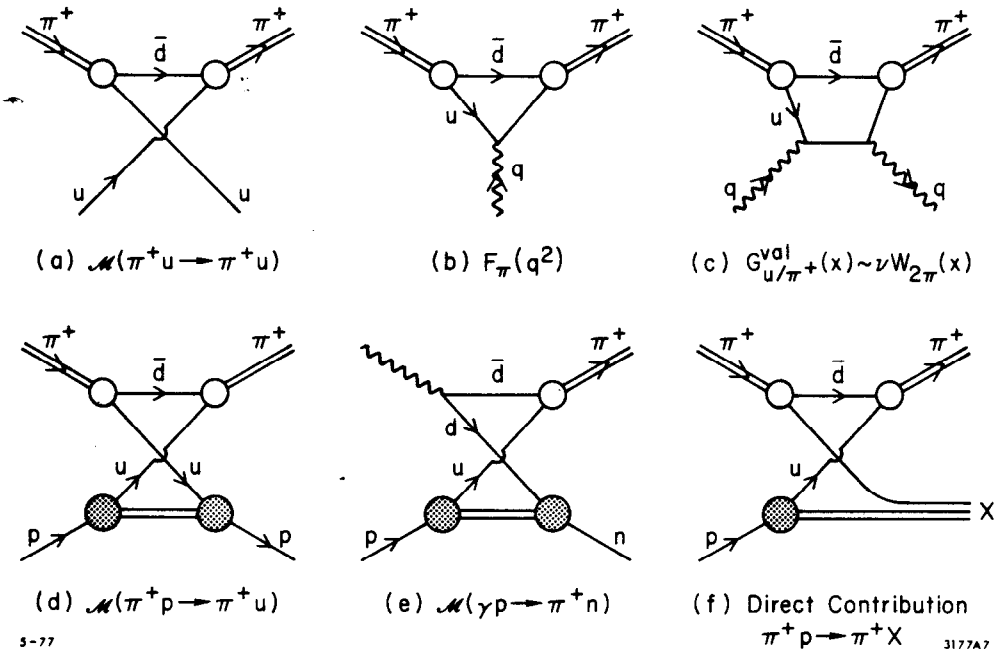

Fig. 3. Contribution of the $\pi^+u \to \pi^+u$ valence scattering amplitude (a), to the pion form factor (b), valence structure function (c), large angle $\pi^+p \to \pi^+p$ scattering (d) and inclusive scattering (f) (direct contribution). The relationship of photoproduction (e) to elastic scattering at large angles (d) is also shown.

Compton scattering, to meson-photon production and to meson-baryon scattering. A useful formula, valid for each of these applications at large t and u, is

$$\mathcal{M}(A+B \to C+B) \cong \frac{1}{x}\, \mathcal{M}(A+q \to C+q)|_{\hat{s}=xs,\, \hat{u}=xu,\, \hat{t}=t}\, F_B(t) \qquad (2.1)$$

where the baryon form factor $F_B(t)$ can be computed directly from the $qB \to qB$ amplitude. The value of $x \sim 0.3$ to 0.4 is the mean valence quark light-cone momentum fraction. Note that a sum over coherent amplitudes is understood in Eq. (2.1). In the case of B-B scattering, there are also terms which restore t-u symmetry.

The calculations of the power laws in the CIM agree with the dimensional counting rules[15]

$$F_H(t) \sim t^{1-n_H} \qquad (2.2)$$

$$\frac{d\sigma}{dt}(A+B \to C+D) \sim s^{2-n_A-n_B-n_C-n_D}\, f(\theta_{c.m.}) \qquad (2.3)$$

(where n_H is the number of elementary fields in H), and are generally consistent with large angle experiments for $30^o < \theta_{c.m.} < 150^o$, $|t|, |u| \gtrsim 3$ GeV^2.

In particular, for pp scattering we predict ($z = \cos\theta_{c.m.}$)

$$\frac{d\sigma}{dt} \sim \frac{1}{s^{10}} \frac{1}{(1-z^2)^a} \tag{2.4}$$

with a between 4 and 6. This is in excellent agreement with the best power law fit to the data, $s^{-9.7\pm0.5}$, and its angular dependence ($a_{exp} \sim 5$-7) over a wide range of $\theta_{c.m.}$.[4] Even more crucial, by s-u crossing, the form of Eq. (2.4) is consistent with $d\sigma/dt(\bar{p}p \to \bar{p}p)/d\sigma/dt(pp \to pp) \sim 1/50$ at $\theta_{c.m.} = 90^o$. The angular dependence predicted by the CIM reflects its duality-diagram topological structure. In addition, all Regge trajectories are predicted to fall to finite values at large negative t, e.g., $\alpha(t) \to 0$ for Compton scattering, $\alpha(t) \to 1$ for meson-baryon and $\alpha(t) \to -2$ baryon-baryon scattering. These predictions can also be tested in the triple Regge ($x_L \to 1$) region of inclusive reactions.

In the case of photoproduction, Anderson et al.[16] find $d\sigma/dt(\gamma p \to \pi^o p)|_{90^o} \propto s^{-7.3\pm0.4}$ in agreement with the prediction, s^{-7}. A new measurement of large angle Compton scattering gives[17]

$$\frac{d\sigma/dt(\gamma p \to \gamma p)}{d\sigma/dt(\gamma p \to \pi^o p)} \propto s^b \qquad \text{for} \quad 4 < s < 10 \text{ GeV}^2 \tag{2.5}$$

with $b = 2.1 \pm .6$ indicating that even at relatively low energies the elementary coupling of a photon to the quark current can be discerned from a meson-dominated interaction.

The magnitude of the fundamental coupling constants α_M and α_B can now be determined in a number of ways, e.g., from the ratio $d\sigma/dt(\gamma p \to \pi^+ n)/d\sigma/dt(\pi^+ p \to \pi^+ p)$ (proportional to α/α_M), from the normalization of the valence quark contribution to the structure functions or form factors (determine α_M and α_B), the normalization of $d\sigma/dt(\pi^+ p \to \pi^+ p)/F_p^2(t)$ (proportional to α_M^2), and $d\sigma/dt(pp \to pp)/F_p^2(t)$ (proportional to α_B^2). The various determinations are consistent within the accuracy of the analysis

and yield[14]

$$\alpha_M = \frac{1}{3}\frac{g^2}{4\pi} \cong 1.2\ \text{GeV}^2$$
$$\alpha_B = \frac{1}{3}\frac{h^2}{4\pi} \cong 10\ \text{GeV}^4 \qquad (2.6)$$

within an uncertainty of order 50%.

III. Inclusive Reactions in the CIM

In the CIM, as well as in other hard scattering models, the inclusive cross section for A+B → C+X at large p_T corresponding to a given subprocess a+b→c+d can be written as a convolution over structure functions $G_{a/A}(x_a, \vec{k}_{Ta})$, $G_{b/B}(x_b, \vec{k}_{Tb})$ and the fragmentation function $D_{C/c}(x_c, \vec{k}_{Tc})$, times the square of the matrix element for the subprocesses (see Fig. 4). Caswell, Horgan, and I[18] have recently analyzed exact calculations in ϕ^3 field theory and have verified that the usual approximation of ignoring the k_T fluctuations in the subprocess matrix element and phase space is reliable for $p_T^2 \gtrsim \langle k_T^2 \rangle$ provided one sums over all leading two-body hard scattering subprocesses. The fact that the incident lines are kinematically determined to be off-shell, e.g.,

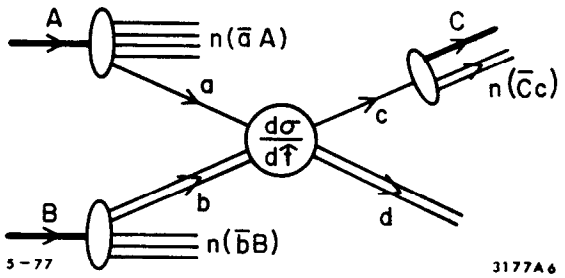

Fig. 4. Hard scattering subprocess contribution ab → c+d to the inclusive cross section A+B→C+X.

$$p_a^2 = -\left[\frac{\vec{k}_{Ta}^2 + m^2(x_a)}{1-x_a}\right] \qquad (3.1)$$

insures that the contribution of diagrams with zero mass exchange contributions are never singular. Although the effect on single particle cross sections is well understood, the k_T fluctuations can still affect p_{out} distributions, correlations with spectators, etc.[19]

It is extremely useful to have an analytic form for the inclusive single particle cross section. If we parametrize

$$\frac{d\sigma}{dt}(a+b \to c+d) = \frac{\pi D}{s^{N-T-U}(-t)^{T}(-u)^{U}} \tag{3.2}$$

and

$$G_{a/A}(x) = \frac{(1-x)^{g_a}}{x} f_{a/A}\,(1+g_a) \tag{3.3}$$

where $f_{a/A} = \int_0^1 dx\, G_{a/A}(x)$ is the (light-cone) fraction of momentum carried by a in A. Then for large p_T, we can write[14]

$$\frac{d\sigma}{d^3p/E}(A+B \to C+X) \cong \sum_{ab \to cd} I\, \frac{(1-x_R)^{F}}{\left(p_T^2\right)^{N}} \frac{1}{(1+x_R z)^{F_+}} \frac{1}{(1-x_R z)^{F_-}} \tag{3.4}$$

where the coefficient is

$$I = D f_{a/A} f_{b/B} 2^{\left(F_+ + F_-\right)} \frac{\Gamma(g_a+2)\,\Gamma(g_b+2)}{\Gamma(g_a+g_b+2)} J \quad , \tag{3.5}$$

and $J(z, x_R)$ is a slow function of $z = \cos\theta_{c.m.}$ and $x_R = p_C/p_{max}$, with $J(0,0) = 1$. The $x_T \to 1$ dependence at 90° is controlled by $F = g_a + g_b + 1$. The angular dependence is controlled by

$$F^- = T + 1 + g_b - N \quad \text{and} \quad F^+ = U + 1 + g_a - N \ .$$

The form (3.4) can be readily generalized to allow for the fragmentation of c into C, taking $D_{C/c}(z) = d(1-z)^f/z$:

$$\frac{d\sigma}{d^3p/E}(A+B \to C+X) \cong (1-x_R)^{f+1} \frac{d\sigma}{d^3p/E}(A+B \to C+X)\, d\, \frac{\Gamma(f+1)\Gamma(F+1)}{\Gamma(f+F+2)} \tag{3.6}$$

We can also allow for a more reasonable shape for $xG_{a/A}(x)$ which gives some flattening at small x:

$$xG_{a/A}(x) = (1+g_a)\, f_{a/A} N_{a/A} \begin{cases} (1-x)^{g_a} & x > \hat{x}_a \\ (1-\hat{x}_a)^{g_a} & x \le \hat{x}_a \end{cases} \tag{3.7}$$

where $N_{a/A}^{-1} = (1-\hat{x}_a)^{g_a}(1+g_a\hat{x}_a)$ and $f_{a/A}$ is still the momentum fraction. The coefficient I is then replaced by $I \cdot N_{a/A} \cdot N_{b/B}$ in Eq. (3.4).

Equation (3.4) is extremely useful, not only for high p_T reactions, but also in calculation of single muons from the Drell-Yan process, inclusive two photon processes reactions $e^-e^- \to C+X$, etc.

The dimensional counting prediction for $G_{a/A}(x)$ at $x \to 1$ is $G_{a/A}(x) \propto (1-x)^{2n(\bar{a}A)-1}$ where $n(\bar{a}A)$ is the number of fast elementary constituents of the bound state A which are left behind after fragmentation. Examples are $\nu W_{2p} \sim G_{q/B} \sim (1-x)^3$, $G_{M/B} \sim (1-x)^5$, $G_{q/M} \sim (1-x)^1$. These predictions are again based on the short distance behavior of lowest order terms in renormalizable perturbation theories assuming a finite Bethe-Salpeter wave function at the origin. (In cases where a is a fermion and A is a boson (or vice-versa) the power can be increased by 1 from spin effects, although this effect is generally cancelled by nonleading corrections. In the case of elementary bremsstrahlung in perturbation theory one has $G_{\gamma/e}(x) \sim \alpha/\pi \log(s/m^2) \cdot (1+(1-x)^2)/x$, etc., where the logarithm arises from the $\vec{k}_T$ integration.) Further discussion may be found in Refs. 11-15.

The result of the convolution and Eqs. (3.4) and (3.6) are all consistent with the counting rules at large p_T and large $\theta_{c.m.}$

$$E\frac{d\sigma}{d^3p}(A+B \to C+X) = \sum_{abcd} \frac{1}{\left(p_T^2+m^2\right)^{n_{active}-2}} f(\epsilon, \theta_{c.m.})$$

$$\underset{\epsilon \to 0}{\sim} \sum_{abcd} \frac{1}{\left(p_T^2+m^2\right)^{n_{active}-2}} \epsilon^F f(\theta_{c.m.})$$

where $\epsilon = 1-x_R = \mathcal{M}^2/s$. Here n_{active} is the number of active fields in the high p_T subprocess (e.g., $n_{active}=4$ for $qq \to qq$, 6 for $qM \to qM$) and $F = 2n_{spect} - 1$ where $n_{spect} = n(\bar{a}A)+n(\bar{b}B)+n(\bar{C}c)$ is the minimum number of elementary constituents that

"waste" the momentum in the fragmentations A→a, B→b, c→C (e.g., $n_{spec}=5$ and F=9 for qq→qq or qM→qM in pp→MX). In general, one predicts that aside from normalization effects, the subprocesses with the minimum n_{active} (minimum p_T^{-1} power) and minimum n_{spect} (minimum F power) will dominate the cross section at large p_T, and small ϵ. Thus, given the fact that the qq→qq term has a small predicted normalization, the dominant terms (for $p_T \lesssim 7$ GeV) for pp→$\pi^{\pm}$, K^+X will come from the qM→qM subprocess (Fig. 5a):

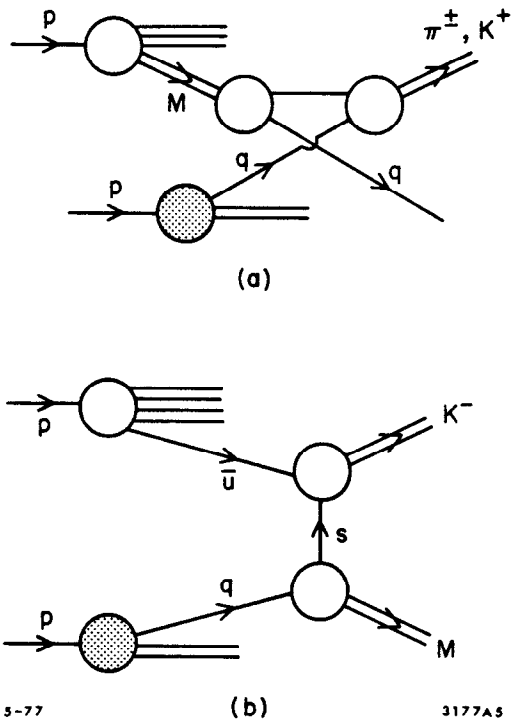

Fig. 5. Dominant CIM contribution to (a) pp→$\pi^{\pm}$, K^+X and (b) pp→K^-X.

$$\frac{d\sigma}{d^3p/E}(pp \to \pi^{\pm}, K^+ X) \sim \frac{\epsilon^9}{\left(p_T^2+m^2\right)^4} f(\theta_{c.m.}) \ .$$

Here m^2 represents terms of order $\langle \vec{k}_T^2 \rangle$, m_q^2, etc. All other quark-hadron subprocesses lead to a higher power of $1/p_T$ or ϵ. In the case of K^- production, the dominant contribution at high p_T small ϵ will come from the "fusion" subprocess $q\bar{q} \to K^-M$ (Fig. 5b)

$$\frac{d\sigma}{d^3p/E}(pp \to K^- X) \sim \frac{\epsilon^{11}}{\left(p_T^2+m^2\right)^4} f(\theta_{c.m.}) \ .$$

A comparison of the CIM predictions with the experimentalists' fits to the Chicago-Princeton-Fermilab[20] data for pp→$\pi^{\pm}, K^{\pm}, p^{\pm}X$ is shown in Table I. The agreement seems remarkable. For example, as shown in Fig. 6, the best fit for the Chicago-Princeton $\theta_{c.m.}=90^0$ data for pp→π^+X is $p_T^{-8.2}(1-x_T)^{9.0}$ (with uncertainties in n and F order ±0.5). The relative suppression of $Ed\sigma/d^3p(pp \to \pi^- X)/Ed\sigma/d^3p(pp \to \pi^+ X) \sim (1-x_T)$

Table I. Scaling predictions for $Ed\sigma/d^3p = C p_T^{-n} (1-x_T)^F$.

Large p_T Process	Leading CIM Subprocess	Predicted	Observed (CP)[20]
		n//F	n//F
$pp \to \pi^+ X$	$qM \to q\pi^+$	8//9	8.2//9.0
π^-	$qM \to q\pi^-$	8//9	8.5//9.9
K^+	$qM \to qK^+$	8//9	8.4//8.8
K^-	$q\bar{q} \to MK^-$	8//11	8.9//11.7
	$qM \to qK^-$	8//13	
$pp \to pX$	$qB \to qp$	12//7	11.7//6.8
$pp \to \bar{p}X$	$q\bar{q} \to B\bar{p}$	12//11	(8.8//14.2)
$\pi p \to \pi X$	$q\bar{q} \to M\pi$	8//5	
	$qM \to q\pi$	8//7	
	$\pi q \to \pi q$	8//3	

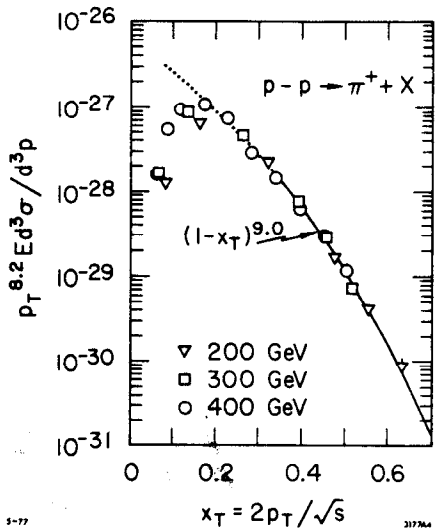

Fig. 6. Scaling law fit to the cross section $pp \to \pi^+ X$, $\theta_{c.m.} \cong 90^\circ$, $x_T = 2p_T/\sqrt{s} > 0.3$. From Ref. 20.

evidently reflects the relative suppression of the d/u quark ratio in the proton structure function at large x.

An important check on the identification of the underlying subprocesses is the angular dependence of its cross section. The leading CIM contribution to $pp \to \pi^+ X$ arises from $u\pi^+ \to u\pi^+$:

$$\frac{d\sigma}{d\hat{t}}(u\pi^+ \to u\pi^+) = \frac{-\pi\alpha^2_M}{\hat{s}\hat{u}^3} = \frac{\pi\alpha^2_M}{\hat{s}^4}\left(\frac{2}{1+z}\right)^3$$

The angular dependence of the subprocess can be determined from experiment either from the

correlated angular dependence of the away side jet[21] or the angular dependence of the $pp \to \pi X$ inclusive cross sections.[6] Analyses indicate that the data are best fit with the form,[6]

$$\frac{d\sigma}{d\hat{t}} \propto \frac{1}{\hat{s}\,\hat{t}^3} \quad \text{or} \quad \frac{1}{\hat{s}\,\hat{u}^3}$$

(equivalent because of the pp symmetry). This coincides with the CIM prediction (1.6a) for the angular dependence reflecting elementary spin 1/2 exchange. It should be emphasized, though, that the phenomenological analyses which use the opposite side jet distribution can be complicated by spectator effects unless the particles in the jet are required to have large p_T.[19]

IV. Normalization of Inclusive Cross Sections

Since the values of the basic quark-hadron couplings α_M and α_B are determined by exclusive processes, predictions of the CIM for inclusive reactions are almost completely constrained: the model predicts the p_T power, $(1-x_R)$ power, and angular shape, as well as the normalization for each contributing subprocess. A complete discussion of baryon-, meson-, and photon-induced reactions will be given in Ref. 14. As an example, for K^+ production in proton-proton collision the dominant CIM subprocesses is $uK^+ \to uK^+$ which contributes (in GeV units) using (2.4)

$$E\frac{d\sigma}{d^3p}(pp \to K^+X) \sim \frac{3(1-x_R)^9}{p_T^8}\left[\frac{1}{(1+x_Rz)^5} + \frac{1}{(1-x_Rz)^5}\right] \qquad (4.1)$$

This estimate is probably accurate to within a factor of 2. In the calculation of the overall normalization we assumed $\alpha_M = 1.2\ \text{GeV}^2$, $f_{u/p} \sim 0.3$ (summed over colors) and $G_{K^+/p} \propto (1-x)^5/x$, normalized to the momentum fraction $f_{K^+/p} \sim 0.1$. We have also included in Eq. (4.1) a factor of ~5 to include the contribution of $uK^+ \to uK^+$, $d\pi^+ \to sK^+$, etc., and a factor of 3 to allow for contribution of decay of resonances into the K^+ from $uK^{+*} \to uK^+ + \pi^0$, etc. This can be compared to the fit to the CP data[20]

at 90^0, $Ed\sigma/d^3p(pp \to K^+X) \cong 5(1-x_T)^{8.4\pm0.5}/p_T^{8.8\pm0.5}$. Thus the normalization of the $qM \to qM$ amplitude as determined from exclusive reactions and form factors is of the right size to account for the FNAL data. The prediction for π^+ is similar but somewhat higher due to the greater number of decay channels.

The leading CIM contribution to K^- production at large x_T is expected to be due to the "fusion" subprocesses $q\bar{q} \to M\bar{M}$. For K^- production this includes $u\bar{u} \to K^+K^-$, $d\bar{u} \to K^0K^-$ as well as K* contributions. Specifically,

$$\frac{d\sigma}{d^3p/E}(pp \to K^-X)\Big|_{90^0} = 0.013\,\frac{(1-x_T)^{11}}{p_T^8} \tag{4.2}$$

for the contribution of the single subprocess $u\bar{u} \to K^+K^-$ alone. The calculation includes a factor of 1/3 from the fact that quarks of the same color must annihilate and 1/2 from the spin crossing factor. Equation (4.2) is useful for an estimate of how often a K^- trigger will be balanced on the away side by exactly one particle, the K^+, in the CIM. We assumed here $\sum_{\text{color}} f_{\bar{u}/p} = 0.03$. Taking all the fusion contributions, the coefficient in Eq. (4.2) is increased to ~0.2. Additionally, one can expect a contribution of order $1.5\,(1-x_T)^{13}/p_T^8$ at 90^0 from $K^-u \to K^-u$ s-channel subprocesses, etc., normalized to ensure $K^-/K^+ \sim 1$ at $x_T \Rightarrow 0$. Thus the fusion subprocesses will not dominate K^- production until $x_T \gtrsim 0.65$.

The value of $\alpha_B \sim 10$ GeV^4 also allows one to predict the normalization cross sections for baryon and antibaryon production. The leading CIM processes are $qB \to q'B'$ and $q\bar{q} \to BB'$. The predictions are consistent with the FNAL and ISR data. Details will be presented in Ref. 14.

V. Charge Correlations in the CIM

It is interesting to see how charge correlations between the trigger charge and the charge of fast particles on the away side arise in the CIM. In the ISR domain, where x_T is small ($\lesssim 0.3$), the dominant CIM subprocesses for K production are

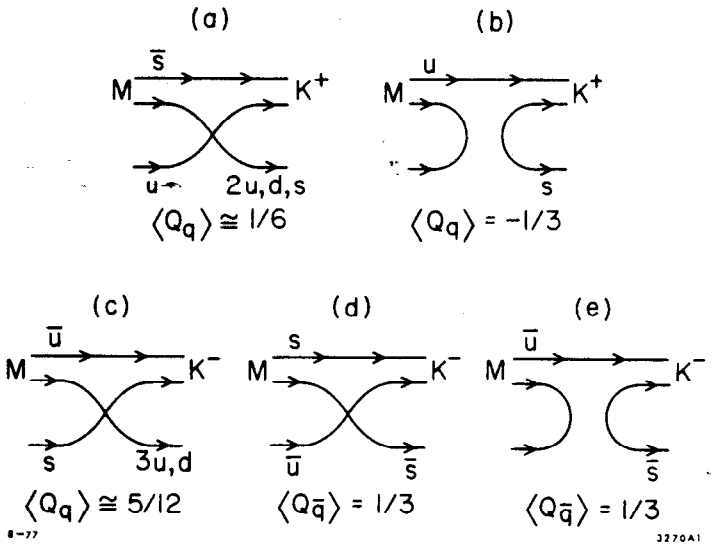

Fig. 7. CIM diagrams for $Mq \to Kq'$.

$qM \to q'K$ and $qM \to q'K^* \to q'K\pi$. The various recoil quark systems q' involved in the direct product of kaons are shown in Fig. 7. (Notice that the strange meson M in 7a is found in the proton Fock state components with ≥ 5 quarks, and the recoil quark has a roughly equal chance (assuming SU(3) symmetry) to be an s or d or either of the two u-quarks.) As shown in the figure the quark system opposite the trigger is always positively charged for a K^-, and roughly neutral (or slightly positive) for the K^+. (The contribution of 7b is suppressed by a factor of 2^4 at 90°.) The same results are maintained when decays of $K^* \to K\pi$ are included. In the case of the fusion contributions, for K^-, the $q\bar{q}$ system tends to have charge 0 or +1, so again the K^- tends to be balanced by positive charge. The charge correlations for p and $\bar{p}$ are predicted to be similar to those for K^+ and K^- triggers, respectively.

Since the CIM processes always involve quark exchange, charge correlations between the trigger and away side systems occur naturally. In contrast, such correlations are generally expected to be small for qq scattering.[3] It will also be interesting to trace the charges of the spectator systems in the beam directions accompanying a high p_T trigger. Also, as emphasized elsewhere,[22] the charge flow associated with massive lepton pair production provides an ideal laboratory for the study of quantum number transfer in high energy reactions.

VI. Jet Production at Large Transverse Momentum

Measurements involving a jet trigger with large total transverse momentum p_T^J are important since the suppression of quark-quark scattering (and other processes involving gluon jets: $Mq \to gq$, $gq \to gq$, $q\bar{q} \to gg$, $gg \to gg$, etc.) from the single particle

trigger bias is removed. It will be crucial to have knowledge of the scaling behavior in p_T^J and x_T^J in order to unravel these contributions.

An important theoretical and experimental question is how to define a large p_T jet trigger which does not confuse contributions from spectator systems. In addition, the large values reported for $<p_T^{out}>$ may indicate contributions from processes involving more than 2→2 collisions. It may be possible to resolve some of these questions by studying a "quark" jet trigger at high p_T^J in deep inelastic lepton scattering where we "know" the subprocess is $\ell q \to \ell q$.

Although the CIM appears to predict the single particle data at large p_T very well, it probably cannot account for the large jet trigger rate seen in the FNAL calorimeter experiment.[9] The dominant jet-trigger contributions in the CIM come from $Mq \to M'q'$ subprocesses giving $d\sigma/d^3p_J/E_J \propto p_{TJ}^{-8}(1-x_{TJ})^9$. In addition there are contributions from other subprocesses $qB \to q'B'$, $q\bar{q} \to M\bar{M}$, $M\bar{M} \to q\bar{q}$, $q+qq \to M+B$ etc. which also provide triggers at high p_T. We estimate that the jet/π^+ rate from CIM terms is probably in the range of 50 to 100 at $p_T = 5$ GeV, $\sqrt{s} = 20$ GeV, and is approximately constant, compared to the measured ratio[9] which is increasing well beyond 300 for $p_T > 5$ GeV. It is possible that $qq \to qq$, $Mq \to gq$, and other elementary quark-gluon contributions could be playing at least a partial role here. These conclusions are tentative, though, in view of the uncertainties in the definition of the jet trigger and the unknown scaling behavior of the data.

The hadronic jets which emerge at large p_T can correspond to other quark, multi-quark, gluon, or hadronic systems and it will be important to have empirical means to discriminate them. The main discriminants are (1) quantum number retention, (2) the leading particle power law behavior at $x = p_L/p_{max}$ near 1, and (3) the associated multiplicity. An interesting possibility is that the magnitude of the hadron multiplicity is directly related to the amount of color separation;[23] in particular the neutralization of a color octet (gluon jet) is predicted to yield 9/4 the multiplicity in the central region

compared to that of a quark jet. Further discussion and references may be found in Ref. 23.

Finally we note that detailed comparisons for various nuclear targets of the jet cross section and the multiplicity at high p_T could be a sensitive tool for uncovering the role of multiscattering in the nucleus.

VII. Conclusions

The experimental data for single particle and jet cross sections, charge momentum, and angular correlations are now so extensive that the constraints on fundamental models have become overwhelmingly restrictive.

If sufficient scale-breaking is assumed—either in the structure functions[24] and/or the scattering amplitude[6]—then it is always possible to interpret the single particle cross sections in terms of an effective quark-quark scattering cross section. However, as we have emphasized here, it is then difficult to understand the strong charge correlations and momentum correlations measured by the BSF collaboration (shown in Figs. 1 and 2), as well as the scale-breaking behavior for baryon production. Further, there is no obvious explanation or connection with exclusive large p_T data.

On the other hand, the constituent interchange model, together with the dimensional counting rules, gives an essentially parameterless description of hadron processes at short distances. The scaling laws of the CIM assume a basic scale-free theory, modulo logarithmic corrections, characteristic of renormalizable perturbation theories. Given that α_s is numerically small and the trigger bias suppression of quark jets, the leading subprocesses for single particle cross sections can then derive from quark-hadron scattering amplitudes. We emphasize that the $qM \to qM$, $qB \to qB$ contributions and their crossing variants are an essential component in any model (including QCD) and that their normalization is fixed by the form factors, the momentum sum rule, etc. The calculated subprocess cross section for $\pi^{\pm}$, or K^+ production in pp collisions is $d\sigma/dt\,(qM \to qM) = \pi\alpha_M^2/su^3$, where α_M is determined by the valence meson wave

function renormalization. This form then yields the observed p_T, $\theta_{c.m.}$, x_T dependence as well as the normalization of the inclusive cross sections. However, as we have discussed in Section VI, it does not seem possible for the CIM to account for the large jet cross section observed at FNAL.

As we have emphasized, processes based on quark-hadron scattering can dominate large-p_T single particle inclusive reactions, despite their p_T^{-8}, p_T^{-12} scaling behavior, due to the absence of trigger bias and the relatively large size of α_M and α_B. We predict the CIM terms will dominate the $qq \to qq$ scale-invariant contributions for p_T below ~7 GeV, assuming $\alpha_s \sim 0.2$. The cross-over point in p_T^2 is controlled by the ratios α_M/α_s and $\sqrt{\alpha_B/\alpha_s}$. For inclusive reactions we also need to estimate the normalization of the $G_{M/B}(x)$ structure functions for virtual $q\bar{q}$ meson-like states, but these can be approximately fixed by normalizing to the measured antiquark momentum fractions. The p_T, $1-x_T$, and angular dependence of inclusive meson and baryon production reactions can then be understood in terms of a minimal set of subprocesses, $qM \to qM$, $qB \to qB$, and their crossing variants. The normalization of each subprocess contribution can be approximately computed, and the theory has a smooth connection to exclusive processes. Detailed predictions for other beams (including photons and leptons) can be made using the simple formula (3.4). There are also many important tests of the model involving correlations between particles on the same side, away side, and beam fragmentation regions. Events are predicted to occur with a single particle in both the trigger and away side systems, via the $q\bar{q} \to M\bar{M}$ and $q\bar{q} \to B\bar{B}$ subprocesses. These will occur at a nonnegligible rate in MB and $\bar{B}B$ collisions.

It is useful to distinguish three regions in transverse momentum for hadronic inclusive reactions at high energies:

(A) The asymptotically scale-free, large p_T region (above $p_T \sim 7$ GeV for single particles, and $p_T \gtrsim 6$ GeV for jets), where the simple perturbation theory contributions for QCD are expected dominate. In this region, in which strong interactions take their

most elementary form, one will be able to study the properties of quark and gluon jets, as well as multiquark jets in the spectator regions.

(B) The moderate p_T zone, where the CIM diagrams are predicted to dominate, giving scaling law contributions of the form p_T^{-8}, p_T^{-12} ... at fixed x_T. In this region (roughly $2 \lesssim p_T \lesssim 7$ GeV for single particles reactions), one can trace the quantum number flow characteristic of duality diagrams. Thus, the dynamical structure of hadrons can be studied in detail in this region. In the case of exclusive reactions, Regge behavior takes its most basic form, with trajectories $\alpha(t)$ receding to negative integers, or in the case of Compton scattering to a J=0 fixed pole.

(C) The most complicated region is at low p_T where the cross sections Feynman-scale and many different coherent, diffractive, Regge, and resonance/cluster phenomena operate. In the central rapidity regions correlations with the quantum numbers of the incident particles become negligible, but the multiplicity in the central region may well be related to the same color confinement dynamics as in $e^+e^- \rightarrow$ hadrons.[23] Furthermore, the fragmentation regions with $x_L = p_L^{c.m.}/p_L^{max} \rightarrow \pm 1$ can also be related to off-shell hadron dynamics, and quark counting rules can be used to discriminate the basic hadronic mechanics at low transverse momentum.[25]

The transition regions between (A) and (B) or (B) and (C) are clearly complicated since several different mechanisms compete, but phenomena in such regions could be important for the study of interference effects, etc. Photon/hadron comparisons are especially important[26]: in regions (A) one predicts $\gamma/\pi \sim$ const at fixed x_T; in region (B) $\gamma/\pi \sim \alpha p_T^2 f(x_T)$.

We note that in the CIM several different areas of hadron phenomenology becomes interconnected: (a) form factors and large t and u exclusive reactions, (b) Regge behavior at large t, (c) the x_L near ± 1 falloff at low t, and (d) large p_T inclusive reactions. The model satisfies the correspondence principle, in the sense of Bjorken and Kogut, and provides a smooth connection between these various regions and phenomena.

Acknowledgments

The work on the CIM reported here was done in collaboration with R. Blankenbecler and J. Gunion. I also wish to thank J. Bjorken, W. Caswell, T. DeGrand, R. Horgan, and N. Weiss for helpful conversations.

References

1. S. M. Berman, J. D. Bjorken, and J. B. Kogut, Phys. Rev. D 4, 3388 (1971). J. Bjorken, Phys. Rev. D 8, 3098 (1973). See also R. F. Cahalan, K. A. Geer, J. Kogut, and L. Susskind, Phys. Rev. D 11, 1199 (1975).
2. R. Møller, XII Rencontre de Moriond, Flaine (1977). H. Bogglid, VIII International Symposium on Multiparticle Dynamics, Kaysersberg, France (1977).
3. We note that such charge correlations might be explained if $q\bar{q} \to q\bar{q}$ or $gg \to q\bar{q}$ annihilation subprocesses play a dominant role. However, calculations in the framework of QCD, as well as crossing symmetry arguments, predict that such contributions are unimportant.
4. Additional references and reviews are given in D. Sivers, S. J. Brodsky, and R. Blankenbecler, Phys. Reports 23 (1976); P. Darriulat, XVIIIth International Conference on High Energy Physics, Tbilisi (1976); S. J. Brodsky and J. F. Gunion, Stanford Linear Accelerator Center preprint SLAC-PUB-1806, op. cit.; S. D. Ellis and R. Stroynowski, Stanford Linear Accelerator Center preprint SLAC-PUB-1903 (1977). See also G. Preparata and M. Rossi, CERN preprint (1976).
5. The relatively small amount of scale-breaking seen in the lepton-pair production continuum cross section and recent deep inelastic neutrino cross sections suggests that such effects probably introduce only logarithmic changes to the large p_T scaling laws. Logarithmic corrections to exclusive dimensional counting rules in an asymptotic freedom theory are discussed by T. Appelquist and E. Poggio, Phys. Rev. D 10, 3280 (1974).

6. R. D. Field and R. P. Feynman, Phys. Rev. D 15, 2590 (1977); R. D. Field, R. P. Feynman, and G. C. Fox, CALT-68-595 (1977).

7. D. Sivers and R. Cutler, Argonne preprint (1977). B. Combridge, J. Kripfganz, and J. Ranft, CERN preprint (1977).

8. However, as emphasized by the authors of Ref. 7, the jet cross section in QCD could be increased by more than an order of magnitude if gluon-gluon and gluon-quark scattering terms are included. (Note that the quark coupling strength "e_g" is effectively 3/2 the quark coupling strength "e_q" in SU(3) color; e.g., $d\sigma/dt\,(gg \to gg) = (81/16)\, d\sigma/dt\,(qq \to qq)$ for $s \gg t$. (See Ref. 23.)) The estimates for gluon contributions are based on the assumption that the structure function for gluons in the proton $G_{g/p}(x)$ should be normalized to $\sim 1/2$ the proton momentum. This may be an over-estimate since gluon emission by a color singlet is suppressed, at least at low x. In the color radiation model of Ref. 23, the large amount of gluon emission in deep inelastic scattering is due to the dynamical separation of quark charges at large $s = (q+p)^2$, rather than the intrinsic presence of gluons in the proton wave function. A detailed discussion will be given elsewhere. We also note that the subprocesses $gq \to Mq$ gives a large $p_T^{-6}\, f(x_T)$ contribution to $pp \to MX$ if $G_{g/p}(x)$ is large. (See Ref. 14.)

9. E. Malamud, VIII International Symposium on Multiparticle Dynamics, Kaysersberg (1977). C. Bromberg et al., Cal Tech preprint 68-590 (1977) and Fermilab preprint CONF-77/62 (1977).

10. In fact, this is an over-estimate since a single gluon does not couple to color singlet states.

11. R. Blankenbecler, S. J. Brodsky, J. F. Gunion, and R. Savit, Phys. Rev. D 8, 4117 (1973); R. Blankenbecler, D. D. Coon, J. F. Gunion, and J. Tran Thanh Van, Stanford Linear Accelerator Center preprint SLAC-PUB-1483 (1974); D. Sivers et al., Ref. 4.

12. R. Blankenbecler, S. J. Brodsky, and J. F. Gunion, Phys. Letters B39, 649 (1972); 42, 461 (1973); Phys. Rev. D 12, 3469 (1975). R. Blankenbecler and S. J. Brodsky, Phys. Rev. D 10, 2973 (1974); J. Gunion, ibid. 10, 242 (1974). Spin corrections are discussed in Sivers et al., Ref. 4. The fusion reactions $q\bar{q} \to M\bar{M}$ have been particularly emphasized by P. V. Landshoff and J. C. Polkinghorne, Phys. Rev. D 10, 891 (1974).

13. For reviews and references see Refs. 4 and 12.

14. R. Blankenbecler, S. Brodsky, and J. Gunion, in preparation. For a preliminary report, see S. Brodsky, R. Blankenbecler, and J. Gunion, XII Rencontre de Moriond (1977) (SLAC-PUB-1938).

15. S. J. Brodsky and G. Farrar, Phys. Rev. Letters 31, 1153 (1973); Phys. Rev. D 11, 1309 (1975). V. Matveev, R. Muradyan, and A. Tavkhelidze, Nuovo Cimento Letters 7, 719 (1973). For a discussion of applications to nuclear systems see R. Blankenbecler, VIII International Symposium on Multiparticle Dynamics, Kaysersberg (1977), and S. Brodsky and B. Chertok, Phys. Rev. 14, 3003 (1976); Phys. Rev. Letters 37, 269 (1976).

16. R. Anderson et al., Phys. Rev. Letters 30, 627 (1973).

17. M. A. Shupe et al. (Tufts-Cornell collaboration), Cornell preprint, to be published.

18. S. Brodsky, W. Caswell, and R. Horgan, in preparation.

19. See R. Wegener, VIII International Symposium on Multiparticle Dynamics, Kaysersberg, France (1977).

20. J. W. Cronin et al., Phys. Rev. D 11, 3105 (1975). M. Shochet et al., XVIIIth International Conference on High Energy Physics, Tbilisi (1976). D. Antveasyan et al., Phys. Rev. Letters 38, 112 (1977). Uncertainties in the n and F values are of order ± 0.5 for $pp \to \pi^{\pm}$, $K^{+}X$, but are much larger for K^{-} and $\bar{p}$.

21. N. Baier, J. Cleymans, K. Kinoshita, and B. Petersson, Nucl. Phys. B118, 139 (1977). N. Baier and B. Petersson, XII Rencontre de Moriond (1977). J. Ranft, op. cit. G. Ranft and J. Ranft, XII Rencontre de Moriond (1977).

22. For a recent discussion of charge retention in quark and multiquark jets and applications, see S. J. Brodsky and N. Weiss, Stanford Linear Accelerator Center preprint SLAC-PUB-1926 (1977), to be published in Phys. Rev.

23. S. Brodsky and J. Gunion, Phys. Rev. Letters 37, 402 (1976). S. Brodsky, XII Rencontre de Moriond (1977) (SLAC-PUB-1937), and references therein.

24. R. C. Hwa, A. J. Speissbach, and M. J. Teper, Phys. Rev. Letters 36, 1418 (1977); R. Hwa, XII Rencontre de Moriond (1977). E. Fischbach and G. Look, Purdue University preprints (1976, 1977). A. P. Contogouris and R. Gasket, McGill preprint (1976). See also E. Levin and M. Ryskin, Yad. Fiz. 18, 1108 (1973).

25. S. Brodsky and J. Gunion, University of California, Davis preprint 77-9, SLAC-PUB-1939 (1977), and references therein.

26. G. R. Farrar, Phys. Letters 67B, 337 (1977), and references therein.